Journal of Institute of Control, Robotics and Systems (2015) 21(3):250-256
http://dx.doi.org/10.5302/J.ICROS.2015.14.0120 ISSN:1976-5622 eISSN:2233-4335

# 시각기반 웜 자세의 기구학적 모형화

# Vision-based Kinematic Modeling of a Worm's Posture

도 용 태*, 탄 콕 키옹
(Yongtae Do[1,*] and Kok Kiong Tan[2])
[1]Department of Electronic & Electrical Engineering, Daegu University
[2]Department of Electrical & Computer Engineering, National University of Singapore

**Abstract:** We present a novel method to model the body posture of a worm for vision-based automatic monitoring and analysis. The worm considered in this study is a Caenorhabditis elegans (C. elegans), which is popularly used for research in biological science and engineering. We model the posture by an open chain of a few curved or rigid line segments, in contrast to previously published approaches wherein a large number of small rigid elements are connected for the modeling. Each link segment is represented by only two parameters: an arc angle and an arc length for a curved segment, or an orientation angle and a link length for a straight line segment. Links in the proposed method can be readily related using the Denavit-Hartenberg convention due to similarities to the kinematics of an articulated manipulator. Our method was tested with real worm images, and accurate results were obtained.

**Keywords:** worm, Caenorhabditis elegans (C. elegans), robot kinematics, Denavit-Hartenberg convention, posture modeling

## I. INTRODUCTION

We propose a novel posture modeling method of a worm using well-defined robot vision technologies. The worm considered in this paper is Caenorhabditis elegans (C. elegans), which is a kind of nematode dwelling in soil. C. elegans has been popularly used in the fields of developmental biology and neurology since Brenner introduced it in 1963 as a model organism for research [1]. The worm is about 1 mm long, has a transparent body, feeds on bacteria, and can be easily and safely cultivated in the laboratory. Although C. elegans has a relatively simple nervous system consisting of 302 well-described neurons, the nervous system exhibits diverse patterns of behavior [2]. C. elegans has a short lifespan of about 2 to 3 weeks, and this is an advantage for research in animal aging. These positive characteristics have made a large number of significant biological findings possible, including findings that won Nobel Prizes (e.g., the discovery of the genetic regulation of organ development and programmed cell death [3]).

In worm studies, human observers often perform time-consuming and labor-intensive analysis of video recordings [4]. However, it is quite difficult for a human to maintain a high level of attention for a large number of images. In addition, behavioral characteristics of worms are practically difficult to characterize manually [5]. To address these practical problems, particularly in the last decade, there have been attempts to develop an automated image analysis system using mature machine vision technologies [5,6]. Using this approach, it is possible to readily acquire the quantitative characteristics of worms over long time periods with little error or ignorance. Baek et al. [7] summarized three advantages of such an automated worm image processing system: (i) the vision-based approach provides a quantitative definition of a particular pattern of worm behavior; (ii) a computerized imaging system can be more reliable at detecting abnormal behavior patterns; and (iii) it is possible to comprehensively assay multiple aspects of a worm's behavior simultaneously.

The first step in vision-based animal behavior analysis is the modeling of the body pose. For nematode worms, a common approach is to represent the body by an open chain of rigid segments [8,9]. However, for a soft, flexible, and long animal such as a worm, the number of segments can be quite large, and this will cause some problems in processing time, algorithm design, and model complexity.

We propose a method that permits both rigid and curved segments to efficiently model the body posture of a worm. Like most existing methods, we approximate the body pose of a worm by connecting some small elements. However, our model accommodates both straight and curved segments. We found that each segment can be characterized simply by two parameters, an angle and a length, whether it is straight or curved, on a two-dimensional (2D) plane. We describe steps to determine the parameters from a worm image. The proposed model can be represented by the Denavit-Hartenberg (D-H) convention, which is often used in robot kinematics [10]. It is well known that other important robot analysis, such as Jacobian and dynamics can be developed mathematically from the kinematics. Associating robot kinematics and worm modeling bridges the gap between two distinct fields - robotics and biology. To the best of our knowledge, the present study is the first attempt to describe a worm using methods from the robotics field.

The rest of the paper is organized as follows. Section II describes some existing methods. Section III presents the proposed modeling method and image processing procedure. Test results obtained are described in Section IV. Finally, our conclusions are given in Section V.

---

* Corresponding Author

Manuscript received November 14, 2014 / revised January 13, 2015 / accepted February 2, 2015

도용태: 대구대학교 전자전기공학부 전자제어공학전공
(ytdo@daegu.ac.kr)
탄 콕 키옹: 싱가포르 국립대학교 전기 및 컴퓨터공학과
(kktan@nus.edu.sg)

※ This work was supported by the National Research Foundation of Korea Grant funded by the Korean Government (NRF-2010-013-D00024).

## II. RELATED WORKS

### 1. Modeling with rigid segments

The first step in the automatic visual analysis of a worm is the modeling of its body. Using a proper model is important because it makes subsequent worm image processing steps (such as position tracking, posture recognition, and type classification) easier and simpler. Huang et al. [8], for example, modeled a worm by connecting a number of rectangular parts, as shown in Fig. 1(a). The position of each part was defined by three values – the coordinates of the center, and the rotation angle of the part. In order to find the best match of the worm model to the binary worm image data, the correspondence between the connected rectangular parts with a smooth worm body was evaluated. The match cost of a part with 12 different possible orientation angles (15°, 30°, 45°, … , 180°) at every possible integer position was computed by convolving the binary worm image with a convolution kernel composed of a match rectangle with different orientation angles. Restif and Metaxas [9] modeled a worm as an open polygon represented by a central body line, and the line is composed of a number of segments and vertices. At each vertex, the local base vectors were defined as the unit vectors parallel and perpendicular to the segment between two adjacent vertices as illustrated in Fig. 1(b). This model follows from the morphology of the worms, which are symmetric along their central body line.

A major problem commonly related to the worm modeling methods described above is the error of the approximation of a soft worm body using rigid segments. In order to achieve high modeling accuracy, the number of segments should be large, but this will increase the complexity of the process. For example, in [9], 100 vertices were sampled to model a small (1 mm long) worm. A further difficulty is that the length of a worm varies while its soft body moves, and rigid segments of the model need to be added or deleted.

### 2. Modeling based on the Denavit-Hartenberg (D-H) convention

In robotics, a manipulator is modeled as a set of rigid links connected in an open-chain by joints. A link is considered to be a rigid body that defines the relationship between two neighboring joint axes. Using the D-H convention [10], the kinematics of a manipulator in three-dimensional (3D) space can be described by specifying the four parameters of each link as defined in Fig. 2: (i) $a_i$ is the link length from $z_i$ to $z_{i+1}$; (ii) $\alpha_i$ is the angle between $z_i$ and $z_{i+1}$ measured about $x_i$; (iii) $d_i$ is the distance from $x_{i-1}$ to $x_i$ measured about $z_i$; and (iv) $\theta_i$ is the angle between $x_{i-1}$ and $x_i$ measured about $z_i$.

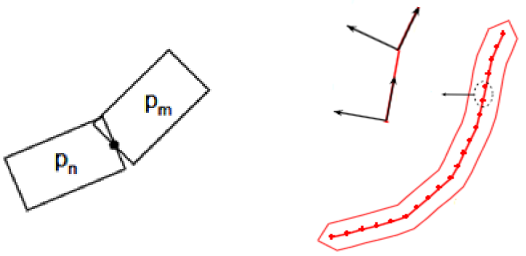

(a) Connected rigid blocks in [8]. (b) Open polygon represented by center line segments in [9].

그림 1. 기존의 웜 모형.

Fig. 1. Existing worm models.

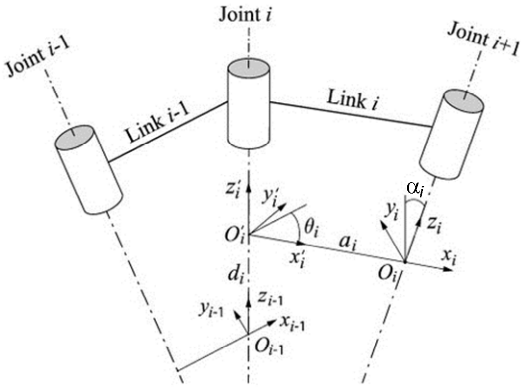

그림 2. Denavit-Hartenberg의 규약.

Fig. 2. Denavit-Hartenberg convention.

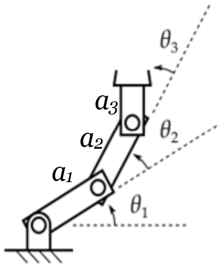

그림 3. 평면로봇의 각 링크는 2개의 인자로 표현가능.

Fig. 3. A link of a planar robot can be represented by two parameters.

If a manipulator is planar, as exampled in Fig. 3 for a robot arm having three degrees of freedom, its kinematics can be described using only two of the four parameters, $a$ and $\theta$, because the other two parameters are always zero. In the existing methods [8,9] described in Section II.1, a worm is modeled as an open-loop articulated chain with rigid segments. This is the same case as that of a robot manipulator that has been modeled as an open chain of multiple solid links [10]. In [11], we used the D-H convention in our analysis of worm images. A worm was parameterized simply by specifying only two D-H parameters, $a$ and $\theta$, when its body was approximated by connected rigid links.

Introducing the D-H convention to the analysis of worm images brings several practical advantages. (i) The posture of a worm can be represented by a few parameters. Particularly, for any planar pose, only two parameters are needed. (ii) There are rich mathematical methods based on the D-H convention in robotics. We can use these mathematical tools readily in the analysis of worm pose and motion. (iii) The use of D-H convention can bridge the gap between two important and distinct fields, robotics and biology. Engineers can help neurologists better understand this tiny but important animal. However, the limitations of existing worm modeling methods by connecting rigid elements have not been resolved. This problem can be overcome if curved links are permitted in the modeling as we propose in Section III.

## III. WORM IMAGE PROCESSING AND CURVED LINK MODEL

The aim of this study is the development of an efficient modeling method with which to describe a worm's body pose. As shown in Fig. 4, a worm is in a smoothly curved posture, and it is natural to suggest that the shape can be better approximated if it is represented with curved links (rather than by many rigid segments). In this section, we describe the processing steps of a worm image and a modeling method that uses curved segments.

A worm image is processed in three steps: detection, filtering and skeletonization. Detecting a worm in an image was achieved by classifying pixels into two classes; the worm and the background. If a worm crawls on a flat agar substrate, the worm and the background will have different brightness in the image due to the rather transparent body of the worm. Thus, binarization was performed in gray level images by comparing image pixel values with a preset threshold.

In the detection process, classification errors can occur - a binary image obtained by thresholding might have holes inside the body region of a worm and blobs in the background of the image. We filtered wrongly classified pixels using two processes. First, morphological operations were applied to remove the holes: dilation (three times) followed by erosion (three times). Secondly, a size filter was applied. Blobs in the image were labeled using different values in order to find their sizes, and small blobs were removed. The 8-connectivity binary image labeling method proposed by Haralick [12] was applied.

The detected image region of a worm was skeletonized so as to effectively represent the body shape of the worm. Fig. 4(b) shows an example of the skeleton image of a worm. Unnecessary branches of the skeleton were pruned to produce a smooth line. The head and tail of a worm can be found by detecting the two end points of the skeleton. When a 3×3 window was scanned over the binary skeleton image $B$, each end point satisfies the following conditions:


(a) (b)

그림 4. (a) 웜 영상 (b) 스켈레톤 영상.

Fig. 4. (a) Worm image (b) Skeleton image.

| | | |
|---|---|---|
| 1 | 0 | 0 |
| 0 | 1 | 0 |
| 0 | 0 | 0 |

(a)

| | | |
|---|---|---|
| 0 | 0 | 0 |
| 0 | 1 | 1 |
| 0 | 0 | 0 |

(b)

| | | |
|---|---|---|
| 1 | 0 | 0 |
| 0 | 1 | 0 |
| 0 | 1 | 0 |

(c)

| | | |
|---|---|---|
| 0 | 0 | 0 |
| 0 | 0 | 1 |
| 0 | 0 | 0 |

(d)

그림 5. 수식 (1)을 사용한 종점 검출의 예: (a)와 (b)는 종점이고, (c)와 (d)는 아님.

Fig. 5. Examples of end point detection using Eq. (1): (a) and (b) are end points, and (c) and (d) are not.

$$\sum_{x=1}^{3}\sum_{y=1}^{3} B(x,y) = 2 \wedge B(2,2) = 1. \tag{1}$$

where $x$ and $y$ are the image coordinates of a pixel. Fig. 5 shows some examples that use Eq. (1).

From the obtained skeleton image of a worm, the worm's body posture was modeled with serially connected link segments. The length of the skeleton $L$ is simply the sum of all pixel values in a binary skeleton image. The joint points that divide the skeleton into $m$ segments of equal length were found at positions where $L/m$ number of pixels were counted along the skeleton from one end point to the other.

The curvedness of each link segment was calculated. We defined the curvedness $\gamma$ by Eq. (2) such that $\gamma$ is zero if the segment is straight, and becomes unity when the link is semicircular with diameter $e$ as shown in Fig. 6.

$$\gamma = \frac{2}{(\pi-2)e}(s-e) \tag{2}$$

where $s$ is the arc length and $e$ is the Euclidian distance between two end points of a segment, as shown in Fig. 7. They can be computed from the $N$ image points constituting the link segment by

$$s = \sum_{i=1}^{N-1}\sqrt{(x_{i+1}-x_i)^2 + (y_{i+1}-y_i)^2} \tag{3}$$

$$e = \sqrt{(x_N - x_1)^2 + (y_N - y_1)^2} \tag{4}$$

If the curvedness $\gamma$ of a link segment is less than an arbitrary threshold, the link is modeled as a straight line segment. A straight line segment can be represented by two parameters: link length $a$ and rotation angle $\theta$. The link length is simply the Euclidean

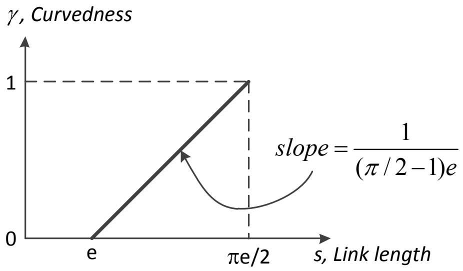

그림 6. 곡률 함수 정의.

Fig. 6. Definition of curvedness function.

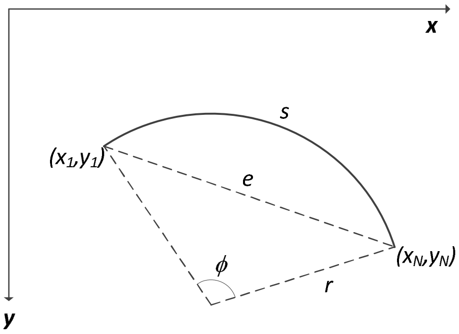

그림 7. 곡선 링크.

Fig. 7. Curved link.

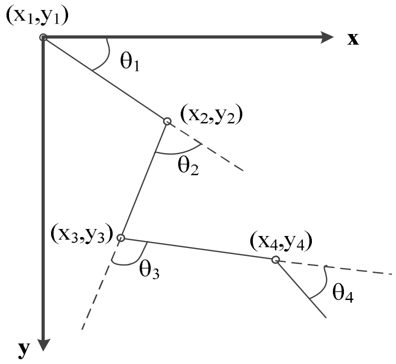

그림 8. 직선 링크의 회전각 $\theta$.

Fig. 8. Rotation angle $\theta$ for rigid links.

distance, and can be calculated in the same way that $e$ is calculated using (4). The rotation angles are computed using *Atan2* (the "arc-tangent two" function). In a rigid planar link connection, as shown in Fig. 8, the rotation angles are computed by

$$\theta_i = A\tan 2(y_{i+1} - y_i, x_{i+1} - x_i) - \theta_{i-1} \quad \text{for} \quad i > 0 \tag{5}$$

where $\theta_0 = 0$.

If a link is curved (i.e., a sufficiently large value of $\gamma$), the conventional modeling method that assumes only rigid segments will result in error. The error can be reduced by increasing the number of connected rigid segments, but dealing with many segments will bring other difficulties such as higher complexity, more storage requirements, and a longer processing time. To overcome this problem, we expanded the link model to accommodate arcs in addition to straight line segments.

For a curved link represented by an arc, we assumed that the arc has a constant curvature and the torsion is zero. Then, the arc can be represented by specifying arc parameters that are determined using the following steps.

A circle of center $(u, v)$ and radius $r$ is represented by

$$(x-u)^2 + (y-v)^2 = r^2 \tag{6}$$

By introducing $g = 2u$, $h = 2v$, and $q = r^2 - u^2 - v^2$, Eq. (6) becomes

$$gx + hy + q = x^2 + y^2 \tag{7}$$

Given $p_i = (x_i, y_i)$, $i=1,2,...N$, image points constituting an arc on a 2D plane, fitting the points are estimated by a least squares fit for the values of $g$, $h$, and $q$ in Eq. (8):

$$\begin{bmatrix} x_1 & y_1 & 1 \\ x_2 & y_2 & 1 \\ \vdots & \vdots & \vdots \\ x_N & y_N & 1 \end{bmatrix} \begin{bmatrix} g \\ h \\ q \end{bmatrix} = \begin{bmatrix} x_1^2 + y_1^2 \\ x_2^2 + y_2^2 \\ \vdots \\ x_N^2 + y_N^2 \end{bmatrix} \tag{8}$$

The arc angle $\phi$ is computed by

$$\phi = s/r = ks \tag{9}$$

where $k$ is the curvature. We can represent any link segment in the model by specifying only two parameters, one for length and the other for angle: $s$ and $\phi$ for a curved link, respectively, or $a$ and $\theta$ for a straight link, respectively.

표 1. 그림 9의 곡선 링크를 위한 D-H 인자.

Table 1. D-H parameters for the curved link shown in Fig. 9.

| Frames | $\theta$ | $d$ | $a$ | $\alpha$ |
|---|---|---|---|---|
| 1 | $\theta_1$ | $0$ | $0$ | $-\pi/2$ |
| 2 | $0$ | $d_2$ | $0$ | $\pi/2$ |
| 3 | $\theta_3$ | $0$ | $0$ | $0$ |

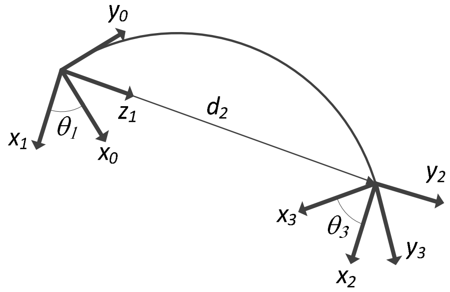

그림 9. 수정 Denavit-Hartenberg 규약[13,14]을 이용한 좌표계 변환.

Fig. 9. Frame transformation using the modified Denavit-Hartenberg convention [13,14].

The proposed modeling method can be analyzed using the D-H convention. A geometric description of the curved link shown in Fig. 7 can be redrawn by considering two frames that are attached at both ends of an arc, as shown in Fig. 9. Using the modified D-H convention that was originally proposed for continuum-style robots [13], the transformation between the two frames can be described by three coupled movements: (i) rotation by an angle $\theta$; (ii) translation by a distance $d$; and (iii) rotation again by angle $\theta$. Here, the rotation angle $\theta$ can be computed by [14]

$$\theta = ks/2 \tag{10}$$

A link parameter table for the model is presented in Table 1. Note $\theta = \theta_1 = \theta_3$ when using the modified D-H convention for the coupled motion. The homogeneous transformation matrix $\boldsymbol{A}$ for a curved link is written from the table as follows:

$$A_0^3 = \begin{bmatrix} \cos(2\theta) & -\sin(2\theta) & 0 & -d\sin\theta \\ \sin(2\theta) & \cos(2\theta) & 0 & d\cos\theta \\ 0 & 0 & 1 & 0 \\ 0 & 0 & 0 & 1 \end{bmatrix} \tag{11}$$

This matrix can be rewritten in terms of $k$ and $s$ for a transformation on a 2D plane as

$$A_0^3 = \begin{bmatrix} \cos(ks) & -\sin(ks) & \{\cos(ks)-1\}/k \\ \sin(ks) & \cos(ks) & \sin(ks)/k \\ 0 & 0 & 1 \end{bmatrix} \tag{12}$$

## IV. RESULTS

We tested the proposed modeling method with real worm images [15]. The test images were of a wild-type C. elegans in 24-bit color format with 240×320 resolution. The color images were first converted into 8-bit gray images of the same size. Fig. 10(a) shows an example worm image. We detected pixels belonging to

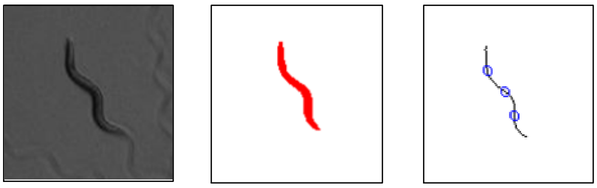
(a) Original image. (b) Detected binary image. (c) Skeleton image divided into four links.

그림 10. 직선 혹은 곡선 링크의 연결에 의한 웜의 자세 모형화.

Fig. 10. Modeling a worm posture by connecting linear or curved links.

the worm in the image by thresholding, as done by Baek et al. in [7]. We used a 5×5 scanning window, and the mean and standard deviation of the pixel values inside the scanning window were calculated at every pixel position. A pixel was decided to be part of a worm body if the mean was less than 80% of the background intensity and the standard deviation was larger than 20% of the mean value. In an image taken using a microscope, pixels in the center region are usually brighter than those at the image boundary. Thus, an image was divided into two regions: the center region 30 pixels away from the image boundary, and the remaining outer region. Different threshold values were applied to the two regions for the detection. After processing the morphological and size filtering steps, we obtained a binary image as shown in Fig. 10(b). Its skeleton was obtained as shown in Fig. 10(c), and the skeleton was divided into four connected links of the same length so as to represent the worm body as an open chain of the links. In the figure, the three connecting joints between the four links are marked by small circles. A link was modeled as an arc if its curvedness $\gamma$ was higher than 0.15. Otherwise, the link was modeled as a straight line segment. The modeling results are shown in Table 2, where link 1and link 2 are modeled as a line, and link 3 and link 4 are represented by an arc.

In order to analyze the performance of the proposed method quantitatively, a modeling error $E$ is defined by the average of the shortest distances between skeleton image points and their link model as follows:

$$E = (1/L)\sum_{i=1}^{m}\sum_{p\in B}|p_i - M_i| \tag{13}$$

where $p$ is any of $L$ points constituting a binary skeleton image $B$ that is divided into $m$ link segments of equal length, and $M$ is a corresponding link model. Here, $M$ is either a line segment or a circular arc, whereas existing methods such as those presented in [9,11] use only a line segment model. The proposed method was tested with nine randomly selected images, and we obtained results as shown in Table 3. A worm was modeled by four link segments, and a link was represented by an arc if its curvedness was larger than 0.15. The proposed method resulted in significantly increased accuracy for all cases when compared with existing methods using only rigid elements. In order to see the effect of the number of link segments on the accuracy, we performed a test with varying link numbers for image No. 1 of Table 3. The test results are shown in Fig. 11. The proposed method showed a consistent accuracy (except for the case of $m$=2) of about 0.5 [pixel] whereas the accuracy of the existing method depends greatly on the number of link segments. The compared method produced similar accuracy to the proposed method when the worm body was segmented into more than seven links. Test results for all images of Table 3 are given in Table 4. The existing modeling method needed 7 to 17 rigid link segments to reach the accuracy obtained by the proposed method which uses only 4 links.

표 2. 그림 10의 웜에 대한 링크 인자. 임의의 링크 세그먼트는 곡률 ($\gamma$)에 따라 직선 ($L$), 또는 곡선 ($C$)으로 모형화된다.

Table 2. Link parameters for the worm shown in Fig. 10. A link segment is modeled as a rigid line ($L$) or a circular arc ($C$) depending on its curvedness ($\gamma$).

| Links | $\gamma$ | *Model* | $\theta$[rad] | $a$ [pixel] | $\phi$ [rad] | $s$ [pixel] |
|---|---|---|---|---|---|---|
| 1 | 0.13 | $L$ | 1.51 | 16.03 | - | - |
| 2 | 0.13 | $L$ | -0.69 | 19.11 | - | - |
| 3 | 0.20 | $C$ | - | - | 1.58 | 19.49 |
| 4 | 0.24 | $C$ | - | - | 1.69 | 18.90 |

표 3. 제안된 방법과 기존 직선 기반 방법[9,11]의 모형화 평균 오차 비교 [단위: 화소].

Table 3. Average modelling error [pixel] comparing the proposed method to existing line-based methods [9,11].

| No. | | 1 | 2 | 3 |
|---|---|---|---|---|
| Image | |  |  |  |
| $\sum_{i=1}^{m}\gamma_i$ | | 0.7057 | 0.7064 | 0.7221 |
| Error | Proposed | 0.5093 | 0.2768 | 0.4649 |
| | Existing | 1.3930 | 1.2558 | 1.4865 |
| No. | | 4 | 5 | 6 |
| Image | |  |  |  |
| $\sum_{i=1}^{m}\gamma_i$ | | 0.6469 | 0.7298 | 0.8270 |
| Error | Proposed | 0.3010 | 0.8483 | 0.2639 |
| | Existing | 1.5683 | 1.6986 | 1.5497 |
| No. | | 7 | 8 | 9 |
| Image | |  |  | 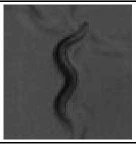 |
| $\sum_{i=1}^{m}\gamma_i$ | | 0.7193 | 0.7362 | 0.7246 |
| Error | Proposed | 0.3051 | 0.7940 | 0.7286 |
| | Existing | 1.4443 | 1.5283 | 1.1620 |

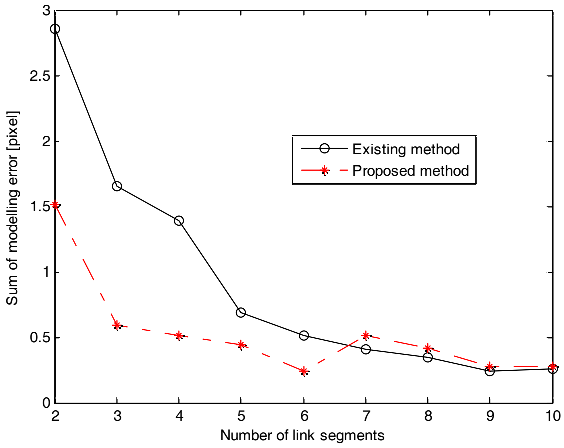

그림 11. 그림 10에 보인 웜 영상(표 3의 1번)에서 링크 세그먼트의 개수에 따른 모형화 정확도.

Fig. 11. Modeling accuracies with different numbers of link segments for the worm image shown in Fig. 10 (No.1 of Table 3).

표 4. 표 3의 각 시험 영상에 대하여 제안된 기법의 정확도를 얻기 위해 요구되는 직선 링크 세그먼트의 개수.

Table 4. Number of rigid link segments required to reach the modeling accuracy of the proposed method for the test images of Table 3.

| Test image | 1 | 2 | 3 | 4 | 5 | 6 | 7 | 8 | 9 |
|---|---|---|---|---|---|---|---|---|---|
| Number of Links | 7 | 11 | 8 | 7 | 10 | 12 | 17 | 13 | 10 |

## V. CONCLUSIONS

We have presented an automated technique to model the body posture of a worm from its image. Our method is based on a four-step processing approach. First, a worm's body is detected from its image by thresholding. Secondly, the image is filtered to remove noise. Thirdly, the body shape is represented by a skeleton image. Fourthly, the skeleton is approximated by connecting curved or line link segments. Unlike most existing methods that connect many rigid line link segments in the model, our method allows both linear and circular arc links. Since the body pose of a worm is smoothly curved, incorporating curved links can be efficient in the modeling, and this is an important contribution of this study. In our experiments, the proposed modeling method showed a consistent accuracy for all test images whereas the accuracy of the compared existing method varied significantly. The compared method needed much more number of link segments than the link number of the proposed method in order to get the accuracy of the proposed method. We introduced detailed techniques of how any link can be efficiently represented by a line segment or an arc segment, and how a link segment can be parameterized. Another important finding is that the proposed method can be readily represented by the D-H convention. By employing the modified D-H convention, which was originally proposed for the kinematic analysis of continuum robots, the linear and curved links can be effectively related. The significance of the use of the D-H convention is that rich theoretical and mathematical tools developed in robotics based on the D-H convention can be applied to the automatic analysis of worms.

## REFERENCES

[1] http://www.wormclassroom.org/short-history-c-elegans-research.

[2] W. Geng, et al., "Automatic tracking, feature extraction and classification of C. elegans phenotypes," *IEEE Trans on Biomedical Engineering*, vol. 51, no. 10, pp. 1811-1820, 2004.

[3] http://nobelprize.org/nobel_prizes/medicine/laureates/2002/press.html.

[4] P. J. Brockie et al., "The C. elegans glutamate receptor subunit NMR-1 Is required for slow NMDA-Activated currents that regulate reversal frequency during locomotion," *Neuron*, vol. 31, pp. 617-630, 2001.

[5] Z. Feng, et al., "An imaging system for standardized quantitative analysis of C. elegans behavior," *BMC Bioinformatics*, vol. 5, 115, 2004.

[6] C. Restif, et al., "CeleST: Computer vision software for quantitative analysis of C. elegans swim behavior reveals novel features of locomotion," *PLoS Computational Biology*, vol. 10, no. 7, e1003702, 2014.

[7] J. Baek, et al., "Using machine vision to analyze and classify C. elegans behavioral phenotypes quantitatively," *Journal of Neuroscience Methods*, 118, pp. 9-21, 2002.

[8] K.-M. Huang, et al., "Automated tracking of multiple C. elegans with articulated models," *Proc. IEEE Int. Symp. Biomedical Imaging*, Arlington, pp. 1240-1243. 2007

[9] C. Restif and D. Metaxas, "Tracking the swimming motions of C. elegans worms with applications in aging studies," *Lecture Notes in Computer Science (LNCS)*, vol. 5241 (Part 1), pp. 35-42, 2008.

[10] Y. Youm, "The role of kinematics in robot development," *Journal of Institute of Control, Robotics and Systems*, vol. 20, no. 3, pp. 333-344, 2014.

[11] Y. Do, "Intelligent worm sorting using robot vision," *Proc. of Int. Symposium on Robotics and Intelligent Sensors*, Kuching, 2012.

[12] R. M. Haralick and L. S. Shapiro, *Computer and Robot Vision*, vol. I, Addison-Wesley, 1992.

[13] M. W. Hannan and I. D. Walker, "Kinematics and the implementation of an elephant's trunk manipulator and other continuum style robots," *Journal of Robotic Systems*, vol. 20, no. 2, pp. 45-63, 2003.

[14] I. D. Walker, "Continuous backbone "continuum" robot manipulators," *ISRN Robotics*, vol. 2013, Article ID 726506, 19 pages, 2013.

[15] http://130.15.90.245/c__elegans_movies.htm

**도용태**

Yongtae Do is a professor in the Division of Electronic & Electrical Engineering at Daegu University. He received the B.Eng, M.E, and Ph.D. degrees all in electronic engineering from Kyungpook Nat'l University, Sogang University, and Hull University, respectively. He has been a visiting professor/scientist to the Robotics Institute at Carnegie Mellon University, University of Wisconsin-Madison, Imperial College London, and Nat'l University of Singapore. His research interests are in the areas of robot vision, AI applications, and sensor systems.

**탄 콕 키옹**

Kok Kiong Tan received his Ph.D. in 1995 from the National University of Singapore (NUS). Prior to joining the university, he was a research fellow at SIMTech, a national R&D institute spearheading the promotion of R&D in local manufacturing industries, where he has been involved in managing industrial projects in IT and automation. He is currently an associate professor with NUS and his current research interests are in Internet applications, remote control and monitoring, precision motion control and instrumentation, advanced process control and autotuning, and general industrial automation.